EPJ Photovoltaics **7**, 70501 (2016)
www.epj-pv.org
DOI: 10.1051/epjpv/2015009

Porous (001)-faceted anatase TiO_2 nanorice thin film for efficient dye-sensitized solar cell

Athar Ali Shah, Akrajas Ali Umar[a], and Muhamad Mat Salleh

Institute of Microengineering and Nanoelectronics, Universiti Kebangsaan Malaysia, 43600 UKM Bangi, Selangor, Malaysia

Received: 14 September 2015 / Received in final form: 18 November 2015/ Accepted: 19 November 2015
Published online: 13 January 2016

Abstract Anatase TiO_2 structures with nanorice-like morphology and high exposure of (001) facet has been successfully synthesized on an ITO surface using ammonium Hexafluoro Titanate and Hexamethylenetetramine as precursor and capping agent, respectively, under a microwave-assisted liquid-phase deposition method. These anatase TiO_2 nanoparticles were prepared within five minutes of reaction time by utilizing an inverter microwave system at a normal atmospheric pressure. The morphology and the size (approximately from 6 to 70 nm) of these nanostructures can be controlled. Homogenous, porous, 5.64 ± 0.002 μm thick layer of spongy-nanorice with facets (101) and (001) was grown on ITO substrate and used as a photo-anode in a dye-sensitized solar cell (DSSC). This solar cell device has emerged out with $4.05 \pm 0.10\%$ power conversion efficiency (PCE) and 72% of incident photon-to-current efficiency (IPCE) under AM1.5 G illumination.

1 Introduction

TiO_2 nanostructure with a larger surface area is ideal for solar cells [1–3], photolysis [4], sensors [5] and photocatalytic applications [4, 6, 7], as it improves the charge-transfer reaction, enhances the redox potential of photogenerated electrons and holes, and reduces the electron-hole recombination. For a solar cell application, TiO_2 with large surface area provides many active centers for reagent adsorption and reaction, improves dye molecules loading and facilitates facile electrolyte diffusion, leads to a facile electron transport in the device [8–12].

In a dye-sensitized solar cell (DSSC), anatase is the TiO_2 polymorph that shows an intriguing performance [13–17]. Since many surface reaction favours to occur at the high-energy site, such as defect, twinning or kinks [18, 19], to synthesize anatase TiO_2 nanostructures having such structural properties promises enhanced performance in applications. Moreover, anatase TiO_2 with high-energy plane, such as (001), and anisotropic-shape (such as nanorice) [20], containing high-surface area and high-defect further promotes active surface reaction and facile electron transfer in the device [5, 21]. Thus, high-performance solar cell or photocatalysis can be obtained from the structure.

In this paper, we present a straightforward method to prepare anatase TiO_2 nanorice with a large-area of high-energy plane of (001) containing high-surface defect via a microwave assisted liquid-phase deposition method. In typical procedure, TiO_2 nanorice (size in the range of 6 to 70 nm) with high-density (thickness of approximately 5.64 ± 0.002 μm) can be successfully grown on an ITO substrate surface via this method using a growth solution containing TiO_2 precursor and hexamethylenetetramine (HMT). The performance of the TiO_2 nanorice in DSSC has been examined. Power conversion efficiency and incident photon to current efficiency as high as $4.05 \pm 0.10\%$ and 72%, respectively, can be achieved so far. The performance of the device could be further enhanced via TiO_2 nanostructure properties as well as device properties improvements. The porous TiO_2 anatase should find a potential used in solar cell and photocatalysis applications.

2 Experimental

2.1 Synthesis and characterization of TiO_2 nanorice on an ITO substrate

The TiO_2 nanorices were synthesized on an ITO substrate by using a microwave-assisted liquid phase deposition method [22–24]. In typical process, the TiO_2 nanorices were prepared by immersing a cleaned ITO substrate (sheet resistance ca. 9–22 Ω/cm^2 purchased from VinKarola instuments USA) which was previously cleaned via an ultrasonication for 30 min in acetone

[a] e-mail: akrajas@ukm.edu.my

and ethanol into a 10 mL of aqueous solution containing equimolar (0.05 M) solution of ammonium hexafluoro titanate ($(NH_4)_2TiF_6$) (AHT) and hexamethylenetetramine (HMT). Both chemical reagents were purchased from Sigma-Aldrich, USA, and used directly without any purification process. To obtain an optimum porosity properties and high percentage of (001) lattice plane of anatase TiO_2, the HMT concentration was varied from 0.03 to 0.08 M. In this case, the TiO_2 precursor molarity was fixed at 0.05 M. The growth time was 5 min, meanwhile the microwave power used was 180 W. After a growth process, the sample was taken out from the solution and rinsed with copious amount of pure water and dried under a nitrogen gas flow. Finally, the substrate was annealed in air at 350 °C for an hour.

Field Emission Scanning Electron Microscope (FESEM) technique (ZeiSS SUPRA 55VP) was used for examining the surface morphology of the sample. Meanwhile, the crystallinity of the nanostructure was examined via a high resolution transmission electron microscopy (HRTEM) analysis using Ziess Libra 200FE HRTEM apparatus operating at 200 kV. The X-ray diffraction spectroscopy (BRUKER D8 Advance with CuKα radiation and scan step as low as 2°/min) and the UV/VIS spectrometer (Lambda 900 Perkin-Elmer) were used to confirm the structure and the phase, and the optical properties of the sample, respectively.

2.2 Fabrication of dye sensitized solar cell and characterization

DSSC with a structure of ITO|TiO_2:dye|electrolyte|Pt electrode was fabricated utilizing the TiO_2 nanorice as the photo active layer. Prior to the device fabrication, a TiO_2 nanostructures modified-ITO substrate was immersed into a 0.05 mM ethanolic solution of dye (N719, purchased from Sigma-Aldrich, USA) for 12 h. It was then gently rinsed with ethanol and dried using a flow of nitrogen gas. For simplicity, we called this structure as as photoanode. A counter electrode was prepared by depositing a platinum layer of approximately 150 nm thickness on glass substrate via a sputtering method. A DSSC was assembled by clamping a photoanode and a counter electrode together. An iodide/tridiode redox couple (Iodolyte AN-50, purchased from Solaronix Switzerland) was used as the electrolyte and injected into the space between the photoanode and Pt counter electrode. The active area of the DSSC device was controlled at 0.24 cm^2.

The photovoltaic responses (I-V and incident photon to current efficiency (IPCE)) of the DSSC device was evaluated using a Keithley high-voltage source-measure unit (SMU) model 237 under AM 1.5 simulated irradiation (100 mW/cm^2) provided by 150 W Newport low-cost solar simulator. The photovoltaic properties of the DSSC device was characterized via an electrochemical impedance spectroscopy method using Solartron 1260 under a frequency range of 0.01 to 1 MHz, bias voltage at 0.5 V, and alternating current amplitude of 50 mA. The current amplitude is required to be higher in this case to accelerate the response and to avoid electrolyte drying during the measurement. However, our device is stable at this high-current source.

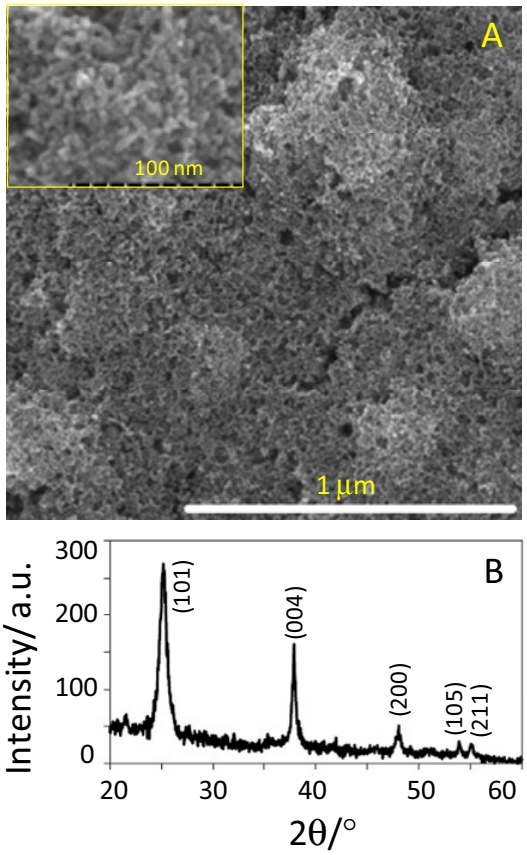

Fig. 1. (A) Typical FESEM image of TiO_2 nanorice grown on an ITO substrate prepared using a growth solution containing 0.05 M of ammonium hexafluoro titanate (AHT), and 0.08 M HMT. Inset shows detailed structure of nanorice. (B) XRD pattern of the TiO_2 nanorice on ITO substrate.

The performance of the samples in the DSSC device was verified at least for five times and the uncorrected standard deviation of the measurement was used to validate the performance of the device.

3 Results and discussion

3.1 TiO_2 nanorice characterization

TiO_2 nanorices have been successfully grown directly on an ITO substrate using the present approach after following a growth process for 5 min in a growth solution containing ammonium hexafluoro titanate (AHT) and hexamethylenetetramine (HMT). In the typical process, TiO_2 nanorice with length-scale from 6 to 70 nm were formed on the surface of ITO with a thickness can be up to 6 μm. Figure 1A shows typical FESEM image of the TiO_2 nanorice prepared using equimolar, i.e. 0.05 M, solution of AHT and HMT. As Figure 1A shows, high-density networked-TiO_2 nanorice forms on the surface covering the entire

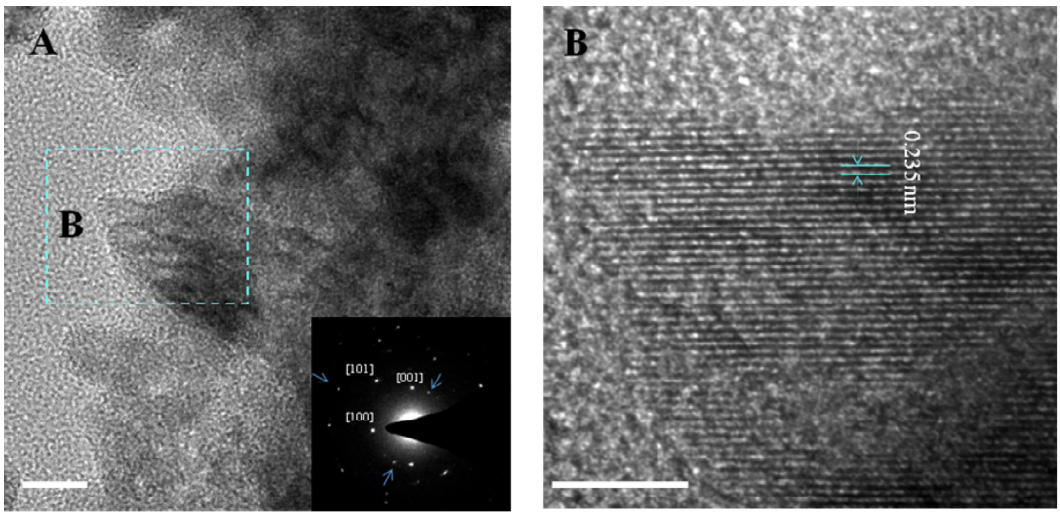

Fig. 2. (A) Low resolution, and (B) high resolution transmission electron microscope images of TiO_2 nanorice. The low resolution image verify nanorice morphology, and as well as SAED analysis (see inset in (A)), showing that nanorice are mono-crystalline. The high resolution image shows fringe spacing of 0.23 nm, reveals high exposure facet (001) with its growth along the [001] direction. Scale bars 10 nm in (A), and 5 nm in (B).

area of the substrate. Such networked-nanostructure produces a TiO_2 nanostructure films with a highly porous property (see inset in Fig. 1A), which is potential for solar cell application due to facilitating a high-dye loading and a facile diffusion of redox species on the surface of the nanostructure. As have been mentioned earlier, the networked-nanostructure is composed of nanoparticles with morphology resembles the rice shape. Probably due to a process of surface energy minimalization, they are connected each other, reflecting the individual TiO_2 nanorice bounded by a high-energy lattice plane. Figure 1B shows the corresponding X-ray diffraction spectrum of the samples. By comparing with the standard powder diffraction file for anatase TiO_2 (JCPDS file no. 21-1272), the obtained result is confirmed to be an anatase polymorph of TiO_2. By comparing with the JCPDS file, the TiO_2 nanorice's XRD spectrum peaks can be labeled as (101), (004), (200), (105) and (211) for peaks at 2θ of 25.5, 37.8, 48.2, 54.0 and 55.0°, respectively. One important fact that can be noted from the result is the peaks ratio between (004) and (101) is quite high, i.e. 0.7, which is much higher compared to normal anatase nanostructure (approximately ranging from 0.2 to 0.4). This reflects that the anatase TiO_2 nanorice is characterized by dominant (001) lattice plane, the second highest in the surface energy. Thus, we expect that enhanced performance in applications, such as solar cell and photocatalysis, can be obtained from this new TiO_2 nanostructure.

The TEM analysis of TiO_2 nanorice structure is presented in Figure 2. A low resolution TEM image shown in Figure 2A verifies the morphology attained by FESEM results. A high resolution TEM analysis highlights the defect-less, smooth, and twinning-less lattice fringes with a spacing approximately 0.235 nm (see Fig. 2B), which reveals that the nanorice are single crystalline in nature, with their unidirectional growth on ITO substrates. This fringe spacing is corresponding to the facet (001), which is in a good agreement with the XRD results. The selected area electron diffraction (SAED) analysis of the nanorice (see inset in Fig. 2A) suggests an overlapping of two TiO_2 nanorice structures, which is depicted by two sets of bright spots, one of them is with high brightness (indexed diffraction pattern) and another with low brightness (pointed with arrows). The brighter set seems to be correspondent to the crystal at the top. The dimmer set can be correspondent to the crystal of TiO_2 nanorice placed at the bottom, as the image is due to diffraction of low energy scattered electrons or may be due to deviation from exact Bragg conditions, such as tilting of crystal (1–3°) and excitation errors. Nevertheless, it confirms that the nanorice is characterized by (001) high-energy lattice plane. A large exposure of high energy facet (001) can play a prominent role in the applications involving photolysis, catalysis and solar cells.

Under normal liquid-phase deposition method, which uses AHT and boric acid as the growth solution, continuous films of TiO_2 is obtained. In the present approach, while microwave energy applications only play a limited role in modifying nanocrystal growth morphology in the case of ZnO nanostructures [24, 25], in good agreement with the reported result by Parmar et al. [20] the microwave induces an anisotropic crystal growth in TiO_2, particularly nanorice-like morphology. By comparing the results obtained by them, which used acetylacetonate to decouple the hydrolysis and polycondensation of Ti ions with the result presented in this work, we remarked that the microwave energy likely induces an anisotropic stress and strain in the nanocrystallite and promotes the formation of anisotropic nanorice of TiO_2. And in the presence of the surfactant (HMT) here via an effective adhesion of its active amine functional onto the TiO_2 nanocrystallite, presumably on (001) plane, the nanorice of anatase

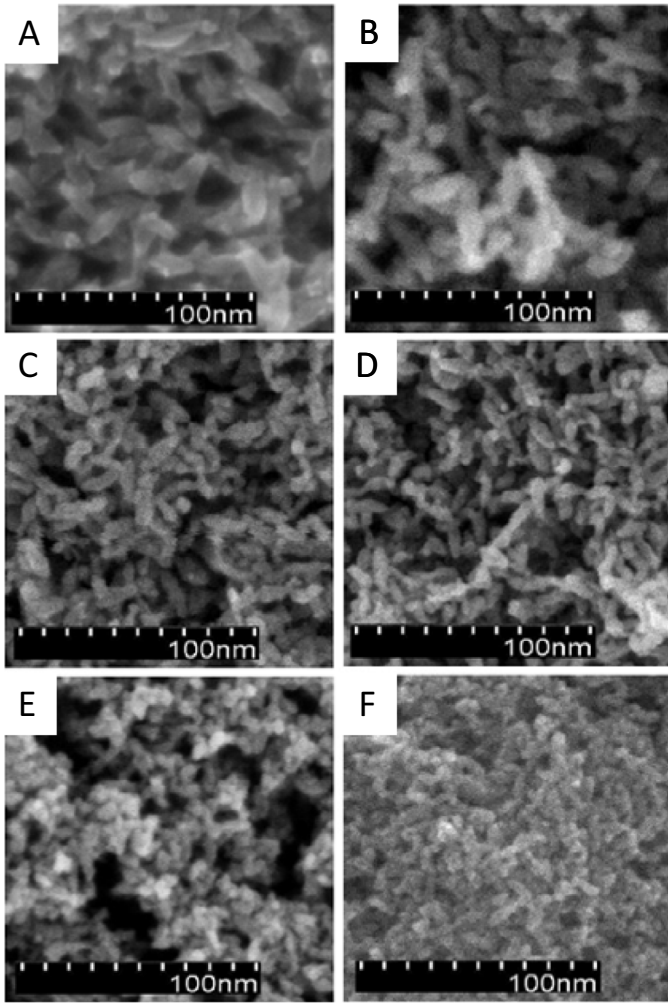

Fig. 3. FESEM of TiO_2 nanorice structures grown on ITO substrate prepared using different HMT concentrations, namely 0.03 (A), 0.04 (B), 0.05 (C), 0.06 (D), 0.07 (E) and 0.08 M (F). $(NH_4)_2TiF_6$ or (AHT) is fixed at 0.05 M. The growth time is 5 min.

TiO_2 that is bounded by this plane is realized. Such feature has also been found in the one-dimensional crystal growth in the case of ZnO [26, 27] and platelet [28, 29], brick-shape [30], nanofibrous [31, 32] and multipods [33] nanocrystal in the case of Au, Pt and Pd. Therefore, in order to obtain the extent role of HMT in the formation of (001)-faceted TiO_2 nanorice, we examined the nanocrystal growth properties under a different HMT concentration. The results are shown in Figure 3. As can be seen from the FESEM results, the length and the diameter of the nanorice decrease with the increasing of HMT concentration. This result reveals that the nature of nanorice packing and density can be controlled on the surface, which the density is increasing with the decreasing of nanorice dimension. Interestingly, from the figure, it was found that, although there is the change in the nanorice dimension, however, the aspect ratio; the length to diameter ratio, was relatively unchanged, namely 2.5. It was also observed that the morphology of the nanorice is unchanged with the

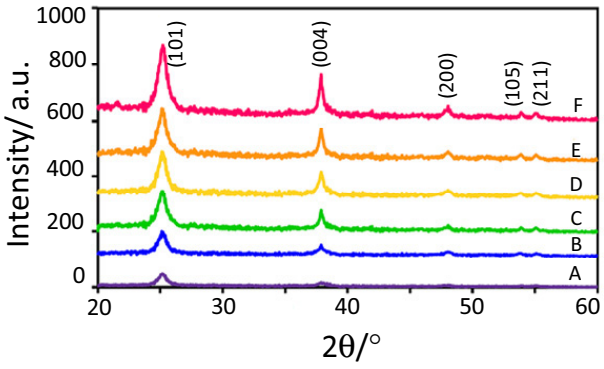

Fig. 4. XRD spectra of TiO_2 nanorice prepared using different HMT concentrations, namely 0.03 (A), 0.04 (B), 0.05 (C), 0.06 (D), 0.07 (E) and 0.08 M (F). AHT was fixed at 0.05 M.

Table 1. TiO_2 nanorice prepared using different HMT concentrations with AHT fixed at 0.05 M.

S. label	HMT(M)	Length (nm)	Width (nm)
A	0.03	70	27
B	0.04	45	18
C	0.05	27	11
D	0.06	24	9
E	0.07	20	7
F	0.08	16	6

variation in the HMT concentration. Despite no morphological modification, however, the change in the dimension as well as the nature of nanorice assembly on the surface may have produced novel properties for enhanced-performance in solar cell application. Table 1 summarizes the dimension of the nanorice prepared from several HMT concentrations with AHT concentration was fixed at 0.05 M.

While the morphology of the nanorice is relatively unchanged upon variation of HMT concentration, the crystalline properties of the samples were also evaluated by using the XRD analysis. The result is shown in Figure 4. As Figure 3 reveals, the crystallographic orientation, i.e. the lattice plane preference, is also found to be unchanged with the variation of HMT in the growth solution. Nevertheless, it was found the peaks intensity of X-ray diffraction from prominent lattice plane increases with the decreasing of nanorice dimension (HMT increasing), while, the full-width at half-maximum (FWHM) decreases with the decreasing of dimension. This reflects that the shrinking in the nanorice dimension might have improved the surface area of particular lattice plane. Thus, novel and enhanced properties are expected to be produced from the nanostructures. Figure 5 shows the optical absorption spectra of the samples shown in Figure 3. In good agreement with the XRD results, the absorbance of the nanorice film effectively increases with the decreasing of the nanorice dimension. Judging from the FESEM results as shown in Figure 3, the increasing in the absorbance upon the decreasing in the nanorice dimension is resulted from the improvement of nanorice assembly, namely become more compact if the nanorice dimension reduces.

Table 2. Photovoltaic parameter of DSSCs device utilizing TiO_2 nanorice with nanograin size variation.

Device	Conc. AHT: HMT (M)	V_{oc} (V)	IPCE	J_{sc} (mA/cm^2)	R_{CT} (Ω)	R_S (Ω)	η (%)	FF
A	0.05:0.03	0.56 ± 0.023	9	1.58 ± 0.24	1014.52	42.39	0.32 ± 0.055	0.36 ± 0.004
B	0.05:0.04	0.62 ± 0.009	34	9.95 ± 0.18	587.15	42.46	2.41 ± 0.14	0.39 ± 0.004
C	0.05:0.05	0.64 ± 0.01	42	13.5 ± 0.22	405.36	40.62	3.24 ± 0.055	0.38 ± 0.004
D	0.05:0.06	0.68 ± 0.01	54	15.34 ± 0.27	307.74	38.9	3.73 ± 0.037	0.4 ± 0.004
E	0.05:0.07	0.68 ± 0.01	61	14.87 ± 0.20	268.81	33.88	3.81 ± 0.033	0.4 ± 0.006
F	0.05:0.08	0.64 ± 0.01	70	16.67 ± 0.265	224.27	34.76	4.05 ± 0.10	0.38 ± 0.004

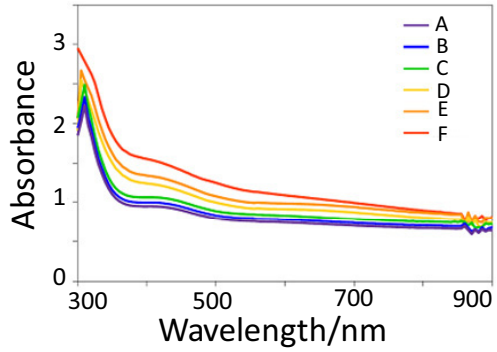

Fig. 5. Typical optical absorption spectra of TiO_2 nanorice prepare using different HMT concentrations.

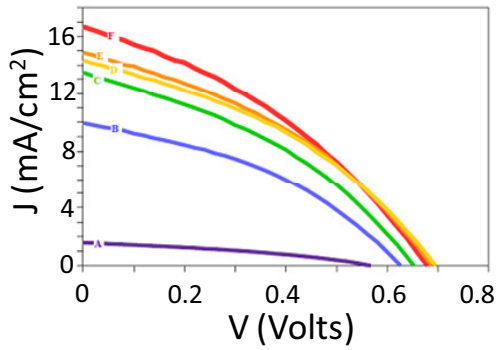

Fig. 6. *J-V* characteristic of the DSSCs utilizing photoanodes with different nanograin size, namely bigger grain size (A) to smaller (F), under A.M1.5, 100 W illumination.

A blue shift is also observed for the samples when the nanorice dimension reduced, which leads to the improvement of open-circuit voltage of the DSSC device [6]. Because of the nanorice assembly become more compact as the dimension reduced and considering the surface area of high-energy lattice plane increase, enhanced photoactivated surface reaction or charge-transfer [25] will be produced as the absorbance of the nanorice film increases with the decreasing of their dimension.

3.2 Solar cell characterization

A DSSC device with structure of ITO|TiO_2: dye (N719)|electrolyte (I^{3-}/I^{2-})|Pt was fabricated to evaluate the photovoltaic property of the new structure. Figure 6

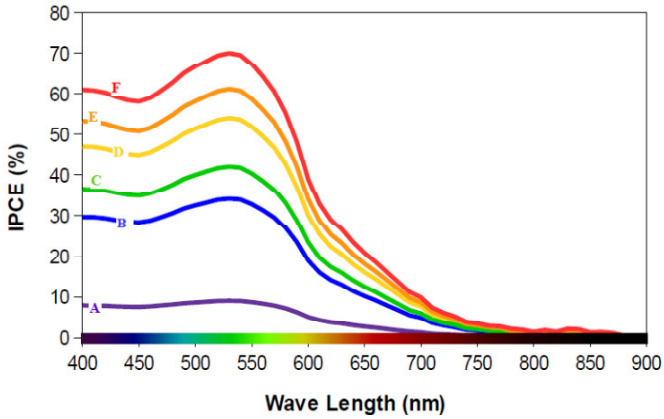

Fig. 7. Incident photon to current efficiency of the devices under A.M1.5, 100 W illumination.

shows typical *J-V* curve for the DSSC device that were fabricated using six different TiO_2 nanorice structures of which their images are shown in Figure 3. As can be seen from Figure 5, the DSSC performance increases with the decreasing of the nanorice dimension, for example, the short-circuit current density (J_{sc}) and the open circuit voltage (V_{oc}) of the device enhanced from 1.58 ± 0.24 mA/cm^2 and 0.56 ± 0.023 V for the high grain size nanorice (device A) to 16.67 ± 0.265 mA/cm^2 and 0.64 ± 0.00 V for small grain nanorice (dimension) (device F). The increase in the performance of the device with the decreasing of nanorice grain size can be attributed to the high photon absorption by the device and possible enhanced electron transport [34,35] as well as facile dye-TiO_2 charge transfer as the increase in the nanorice density and the surface are of high-energy (001) plane. The variation in the performance of the DSSC upon the variation of the nanorice size is unlikely related to the effect of surfactant because of the surfactant is seemed to be removed upon post-growth annealing at 350 °C for one hour. Therefore, it is clearly associated with the variation in the nanorice surface physico-chemistry. The photovoltaic parameters of the devices are summarized in Table 2.

IPCE responses of the devices as shown in Figure 7 further verifies such phenomenon. The increasing value of IPCE of the device with the reducing of nanograin size stamped the role of high energy facet (001) exposure to generate photo electrons, and facilitates facile electron transportation. Hence, J_{sc} is enhanced. As can be seen from Figure 5, the V_{oc} of the device increases

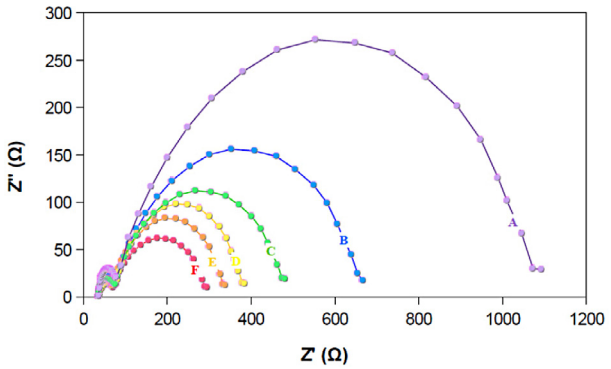

Fig. 8. Electrochemical impedance spectra (EIS) of the devices.

as the nanograin size decreases, reflecting the increasing of exciton lifetime or limited electron-hole recombination. Nevertheless, the device 'F' (device with the smallest nanograin size) shows a slight falls in V_{oc}, which can be attributed to the increasing of electron-hole recombination's rate [17, 36]. In spite of that fact, the device 'F' exhibits significant rise in J_{sc}, the result of enhanced exciton formation and facile electron transportation in the device probably due to greater exposure of high energy surface area.

Electrochemical impedance spectroscopy (EIS) study of the devices (A-F) has explained such transportation of electrons and electron-hole recombination's natures in the device. The results are shown in Figure 8. It is observed that device 'A' with high V_{oc} but low in fill factor, IPCE, and current density has higher value of charge transfer resistance (R_{CT}) in the region of Dye: TiO_2|electrolyte interface, when compared with other devices 'B–F', rendering higher rate of recombination and weak charge transportation [2]. This is due to less reactive of (001) facet because of bulkier dimension. The R_{CT} decreased to a great extent when the nanograin size reduce, as per expectation due to more (001) facet exposure. This may improve dye adsorption and interconnection between these nanoparticles [37]. Thus, the PCE increased.

4 Conclusions

Thin films of anatase TiO_2 with nanorice morphology and rich of (001) facet has been successfully synthesized directly on an ITO substrate surface via a liquid-phase deposition method using a growth solution containing hexamethylenetetramine (HMT) and ammonium hexafluoro titanate (AHT) under a microwave irradiation. The size of the nanorice as well as the basal plane of the nanocrystal can be finely controlled by varying the concentration of HMT in the reaction. It was found that the performance of the dye-sensitized solar cell was improved if the fraction of (001) facet in the nanostructures was increased. It was found that the performance of the DSSC device increases with the decreasing of nanorice dimension. The optimum device demonstrates the power conversion efficiency as high as $4.05 \pm 0.10\%$ with internal quantum efficiency (IPCE) as high as 72%. The decreasing in the nanorice dimension is predicted to increase the (001) facet exposure, enhancing the photoactivity, surface reactivity and electron transport in the device.

The authors would like to acknowledge the Ministry of Higher Education (MOHE), Malaysia for funding this work under research grants FRGS/1/2013/SG02/UKM/02/8 and HiCOE Project. The authors are also grateful for the financial support received from Ministry of Science, Technology and Innovation (MOSTI), Malaysia for the funding under Science Fund Grant (06-01-02-SF1157).

References

1. M. Graetzel, R.A.J. Janssen, D.B. Mitzi, E.H. Sargent, Nature **488**, 304 (2012)
2. M. Gratzel, Nature **414**, 338 (2001)
3. A. Ali Umar, S. Nafisah, S.K. Md Saad, S. Tee Tan, A. Balouch, M. Mat Salleh, M. Oyama, Sol. Energy Mater. Sol. C **122**, 174 (2014)
4. A.L. Linsebigler, G. Lu, J.T. Yates, Chem. Rev. **95**, 735 (1995)
5. W.-J. Ong, L.-L. Tan, S.-P. Chai, S.-T. Yong, A.R. Mohamed, Nanoscale **6**, 1946 (2014)
6. H. Ariga, T. Taniike, H. Morikawa, M. Tada, B.K. Min, K. Watanabe, Y. Matsumoto, S. Ikeda, K. Saiki, Y. Iwasawa, J. Am. Chem. Soc. **131**, 14670 (2009)
7. K. Lee, D. Kim, P. Roy, I. Paramasivam, B.I. Birajdar, E. Spiecker, P. Schmuki, J. Am. Chem. Soc. **132**, 1478 (2010)
8. J.R. Jennings, A. Ghicov, L.M. Peter, P. Schmuki, A.B. Walker, J. Am. Chem. Soc. **130**, 13364 (2008)
9. A.J. Frank, N. Kopidakis, J. van de Lagemaat, Coordin. Chem. Rev **248**, 1165 (2004)
10. E.J.W. Crossland, N. Noel, V. Sivaram, T. Leijtens, J.A. Alexander-Webber, H.J. Snaith, Nature **495**, 215 (2013)
11. C. Ducati, Nature **495**, 180 (2013)
12. E.L. Crepaldi, G.J.D.A.A. Soler-Illia, D. Grosso, F. Cagnol, F. Ribot, C. Sanchez, J. Am. Chem. Soc. **125**, 9770 (2003)
13. H. Zhang, Y. Wang, P. Liu, Y. Han, X. Yao, J. Zou, H. Cheng, H. Zhao, ACS. Appl. Mater. Interfaces **3**, 2472 (2011)
14. W.-Q. Wu, B.-X. Lei, H.-S. Rao, Y.-F. Xu, Y.-F. Wang, C.-Y. Su, D.-B. Kuang, Sci. Rep.-Uk **3**, 1352 (2013)
15. N. Wu, J. Wang, D.N. Tafen, H. Wang, J.-G. Zheng, J.P. Lewis, X. Liu, S.S. Leonard, A. Manivannan, J. Am. Chem. Soc. **132**, 6679 (2010)
16. A. Staniszewski, S. Ardo, Y. Sun, F.N. Castellano, G.J. Meyer, J. Am. Chem. Soc. **130**, 11586 (2008)
17. W. Shao, F. Gu, L. Gai, C. Li, Chem. Commun. **47**, 5046 (2011)
18. L.M. Falicov, G.A. Somorjai, Proc. Natl. Acad. Sci. **82**, 2207 (1985)
19. C.-Y. Chiu, P.-J. Chung, K.-U. Lao, C.-W. Liao, M.H. Huang, J. Phys. Chem. C **116**, 23757 (2012)
20. K.P.S. Parmar, E. Ramasamy, J. Lee, J.S. Lee, Chem. Commun. **47**, 8572 (2011)
21. C.-W. Peng, T.-Y. Ke, L. Brohan, M. Richard-Plouet, J.-C. Huang, E. Puzenat, H.-T. Chiu, C.-Y. Lee, Chem. Mater. **20**, 2426 (2008)

22. A.A. Umar, M.Y.A. Rahman, S.K.M. Saad, M.M. Salleh, M. Oyama, Appl. Surf. Sci. **270**, 109 (2013)
23. F.K.M. Alosfur, M.H.H. Jumali, S. Radiman, N.J. Ridha, M.A. Yarmo, A.A. Umar, Nanoscale Res. Lett. **8**, 1 (2013)
24. N.J. Ridha, A.A. Umar, F. Alosfur, M.H.H. Jumali, M.M. Salleh, J. Nanosci. Nanotechnol. **13**, 2667 (2013)
25. S.T. Tan, A.A. Umar, M. Yahaya, C.C. Yap, M.M. Salleh, J. Phys.: Conf. Ser. **431**, 012001 (2013)
26. L. Vayssieres, Adv. Mater. **15**, 464 (2003)
27. S.T. Tan, A.A. Umar, M. Yahaya, M.M. Salleh, C.C. Yap, H.-Q. Nguyen, C.-F. Dee, E.Y. Chang, M. Oyama, Sci. Adv. Mater. **5**, 803 (2013)
28. A.A. Umar, M. Oyama, M.M. Salleh, B.Y. Majlis, Cryst. Growth Design **9**, 2835 (2009)
29. A. Ali Umar, M. Oyama, M. Mat Salleh, B. Yeop Majlis, Cryst. Growth Design **10**, 3694 (2010)
30. A.A. Umar, M. Oyama, Cryst. Growth Design **8**, 1808 (2008)
31. A. Balouch, A. Ali Umar, A.A. Shah, M. Mat Salleh, M. Oyama, ACS Appl. Mater. Interfaces **5**, 9843 (2013)
32. A. Balouch, A.A. Umar, S.T. Tan, S. Nafisah, S.K. Md Saad, M.M. Salleh, M. Oyama, RSC Adv. **3**, 19789 (2013)
33. A.A. Umar, M. Oyama, Cryst. Growth Design **9**, 1146 (2009)
34. Q. Meng, T. Wang, E. Liu, X. Ma, Q. Ge, J. Gong, Phys. Chem. Chem. Phys. **15**, 9549 (2013)
35. M. Harb, P. Sautet, P. Raybaud, J. Phys. Chem. C **115**, 19394 (2011)
36. Z. He, C. Zhong, X. Huang, W.Y. Wong, H. Wu, L. Chen, S. Su, Y. Cao, Adv. Mater. **23**, 4636 (2011)
37. K. Zhu, N.R. Neale, A. Miedaner, A.J. Frank, Nano Lett. **7**, 69 (2007)

Cite this article as: Athar Ali Shah, Akrajas Ali Umar, Muhamad Mat Salleh, Porous (001)-faceted anatase TiO_2 nanorice thin film for efficient dye-sensitized solar cell, EPJ Photovoltaics **7**, 70501 (2016).